Alzheimer's Research & Therapy

RESEARCH

Open Access

Effects of strategic white matter hyperintensities of cholinergic pathways on basal forebrain volume in patients with amyloid-negative neurocognitive disorders

Ye Eun Kim[1], Jae-Sung Lim[1*], Chong Hyun Suh[2], Hwon Heo[2], Jee Hoon Roh[3,4], E-nae Cheong[5], Yoojin Lee[1], Jae Woo Kim[1] and Jae-Hong Lee[1*]

Abstract

Background The cholinergic neurotransmitter system is crucial to cognitive function, with the basal forebrain (BF) being particularly susceptible to Alzheimer's disease (AD) pathology. However, the interaction of white matter hyperintensities (WMH) in cholinergic pathways and BF atrophy without amyloid pathology remains poorly understood.

Methods We enrolled patients who underwent neuropsychological tests, magnetic resonance imaging, and ^{18}F-florbetaben positron emission tomography due to cognitive impairment at the teaching university hospital from 2015 to 2022. Among these, we selected patients with negative amyloid scans and additionally excluded those with Parkinson's dementia that may be accompanied by BF atrophy. The WMH burden of cholinergic pathways was quantified by the Cholinergic Pathways Hyperintensities Scale (CHIPS) score, and categorized into tertile groups because the CHIPS score did not meet normal distribution. Segmentation of the BF on volumetric T1-weighted MRI was performed using FreeSurfer, then was normalized for total intracranial volume. Multivariable regression analysis was performed to investigate the association between BF volumes and CHIPS scores.

Results A total of 187 patients were enrolled. The median CHIPS score was 12 [IQR 5.0; 24.0]. The BF volume of the highest CHIPS tertile group (mean ± SD, 3.51 ± 0.49, CHIPSt3) was significantly decreased than those of the lower CHIPS tertile groups (3.75 ± 0.53, CHIPSt2; 3.83 ± 0.53, CHIPSt1; $P = 0.02$). In the univariable regression analysis, factors showing significant associations with the BF volume were the CHIPSt3 group, age, female, education, diabetes mellitus, smoking, previous stroke history, periventricular WMH, and cerebral microbleeds. In multivariable regression analysis, the CHIPSt3 group (standardized beta [β_{std}] = -0.25, $P = 0.01$), female ($\beta_{std} = 0.20$, $P = 0.04$), and diabetes

*Correspondence:
Jae-Sung Lim
jaesunglim@amc.seoul.kr
Jae-Hong Lee
jhlee@amc.seoul.kr

Full list of author information is available at the end of the article

mellitus (β_{std} = -0.22, $P < 0.01$) showed a significant association with the BF volume. Sensitivity analyses showed a negative correlation between CHIPS score and normalized BF volume, regardless of WMH severity.

Conclusions We identified a significant correlation between strategic WMH burden in the cholinergic pathway and BF atrophy independently of amyloid positivity and WMH severity. These results suggest a mechanism of cholinergic neuronal loss through the dying-back phenomenon and provide a rationale that strategic WMH assessment may help identify target groups that may benefit from acetylcholinesterase inhibitor treatment.

Keywords White matter hyperintensities, Basal forebrain, Neurodegeneration, Cholinergic pathway, Amyloid-negative, vascular cognitive impairment

Background

The cholinergic neurotransmitter system plays a pivotal role in maintaining normal cognitive function, and acetylcholinesterase inhibitors are widely used to mitigate the progression of memory loss [1–3]. White matter integrities in the cholinergic pathways were already reduced in patients with subjective cognitive decline, with more widespread changes in mild cognitive impairment and Alzheimer's disease (AD) dementia [4]. The primary substrate of cholinergic pathways in the central nervous system is the basal forebrain (BF) complex [1, 2, 5]. Cholinergic neuronal loss in the BF was associated with cognitive decline in degenerative dementias such as AD and Parkinson's disease dementia [5]. The cholinergic neurons of the BF were particularly vulnerable to AD pathology, and BF degeneration has been recognized to precede and predict both entorhinal pathology and memory impairment [6–9]. In patients with vascular cognitive impairment (VCI), an association between the cholinergic system and cognitive dysfunction has also been reported [10, 11]. In patients with subcortical VCI, cognitive dysfunction was correlated with the burden of white matter hyperintensity (WMH), corresponding to cholinergic pathway disruption, whereas the association with atrophy of the nucleus basalis of Meynert (nbM) within the BF was not significant, unlike in AD [10, 11]. However, previous studies had small participant numbers and did not identify the impact of strategic WMH alone, independent of amyloid pathology.

This study aimed to investigate the impact of WMH burden in cholinergic pathways on neurodegeneration in the BF independently of amyloid deposition. We hypothesize that a substantial WMH burden on cholinergic pathways would cause cholinergic neuronal loss via a dying-back phenomenon, leading to BF atrophy. We limited our study to patients with negative amyloid positron emission tomography (PET) to exclude any potential confounding effects of β-amyloid pathology on BF neuronal loss [12–14].

Methods

Study design and participants

We conducted a retrospective cross-sectional study of patients who presented to Asan Medical Center in Seoul between January 2015 and February 2022 with cognitive impairment and underwent comprehensive neuropsychological tests (Seoul Neuropsychological Screening Battery [SNSB]), structural brain magnetic resonance imaging (MRI), and ^{18}F-florbetaben amyloid PET for differential diagnosis (Fig. 1). The SNSB assesses five cognitive domains—attention, language and related functions, visuospatial functions, memory, and frontal/executive functions—through a total of 29 subtests, 15 of which provide quantitative evaluations [15]. This battery was standardized on 1,067 cognitively normal individuals aged 45 to 90 years, with normative data considering age and education. The cutoff for cognitive decline was set at a score below −1.5 standard deviations in at least one cognitive domain, based on these norms. Patients with objective cognitive impairment confirmed by comprehensive neuropsychological testing (SNSB) and a negative amyloid PET scan were selected to determine the effect of WMH on BF degeneration. Amyloid PET scans were performed in accordance with the recommendations outlined in the "Appropriate use criteria for amyloid PET." [16] These criteria were summarized as follows: (1) patients with persistent or progressive unexplained mild cognitive impairment (MCI), (2) patients suspected of having AD but presenting atypical clinical course or having mixed etiologies, and (3) patients with early onset dementia. The brain amyloid plaque load (BAPL) score was utilized to assess amyloid positivity, with a score of 1 indicating the absence of amyloid deposits [17]. In addition to the visual grade, we also used a quantitative method to verify the standardized uptake value ratio (SUVR) values. The acquired amyloid PET images were registered with 3D T1-weighted MR images. The voxels in the amyloid PET images were scaled using the mean uptake value in the cerebellar gray matter to compute the mean cortical SUVR using Neurophet SCALE PET (version 1.2, Neurophet, Seoul, South Korea [18]. The cutoff for this SUVR method with cerebellar gray matter as the reference region was 1.43 [19]. Patients diagnosed with

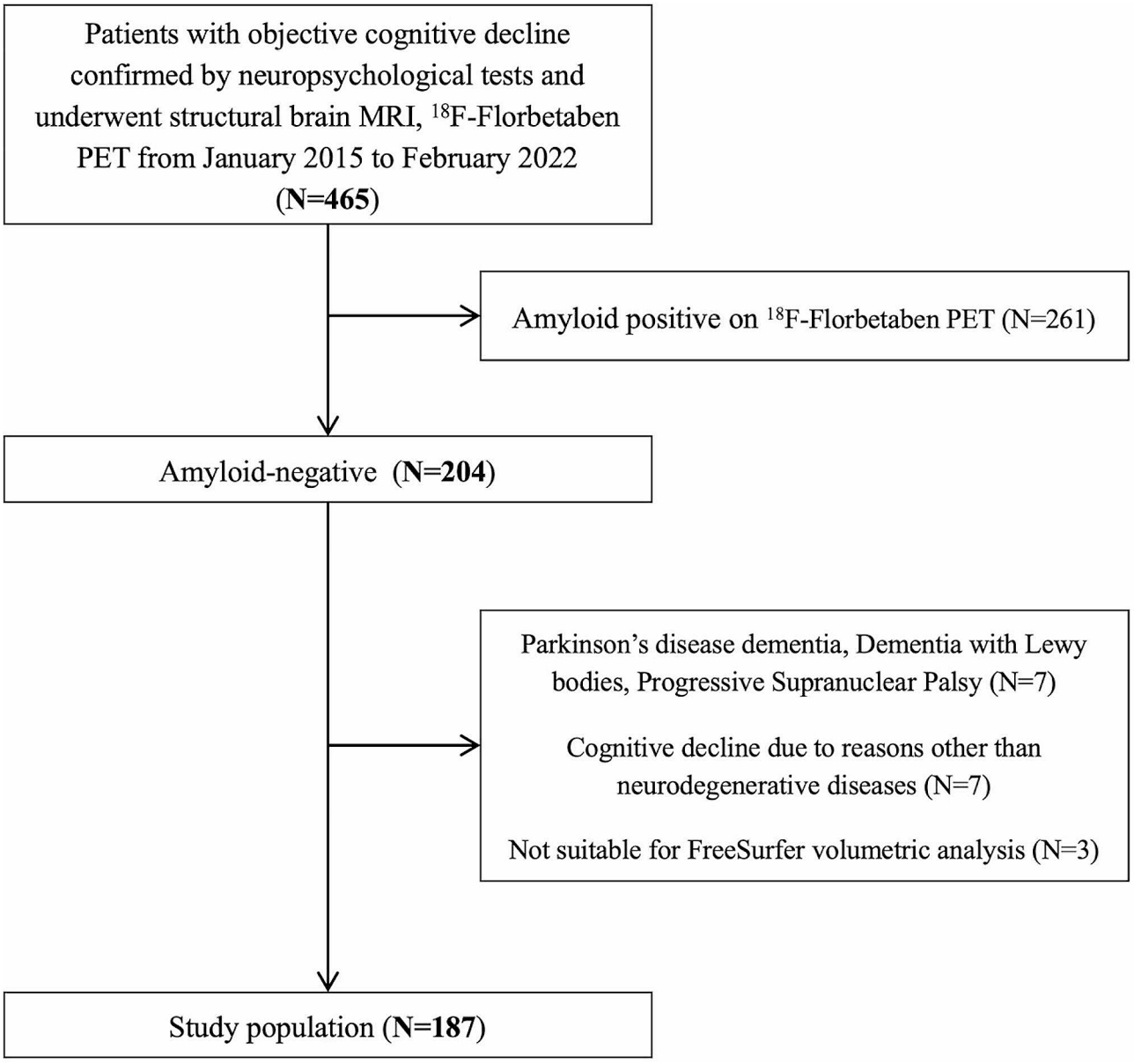

Fig. 1 Enrollment and flow chart of the study participants

Parkinson's disease dementia or dementia with Lewy bodies were excluded from the study as they may have atrophy of the basal forebrain independent of WMH [5]. We also excluded patients with other causes of cognitive impairment, including encephalitis, traumatic brain injury, territorial infarct, and metabolic encephalopathy. We collected data on age at the time of MRI, vascular risk factors including hypertension, diabetes mellitus, hyperlipidemia, coronary artery disease, smoking, as well as stroke history, apolipoprotein E (APOE) ε4 status, baseline Mini-Mental State Examination (MMSE) scores, and detailed neuropsychological test results through electronic medical records. Vascular risk factors, such as hypertension and diabetes mellitus, were defined as taking medication for these conditions, including antihypertensive and antidiabetic drugs, or having a medical record of a diagnosis of these conditions. Due to the study's retrospective nature and the low risk to participants, the local institutional review board approved the protocol and waived patient consent. All methods were performed in accordance with the relevant guidelines and regulations of the Asan Medical Center Ethics Committee and the Declaration of Helsinki.

Acquisition of MRI

MRI images acquired for the differential diagnosis of cognitive impairment in an outpatient setting were collected through a picture archiving and communication

system (PACS). The high-resolution volumetric images were obtained in the sagittal plane with a 3D gradient-echo T1-weighted sequence using a 3-T MRI unit (Ingenia, Philips Healthcare). The detailed parameters were as follows: a TR of 9.6 ms, TE of 4.6 ms, a flip angle of 8°, a FOV of 224×224 mm, a section thickness of 1 mm with no gap, and a matrix size of 224×224. Fluid-attenuated inversion recovery (FLAIR) imaging was obtained using a turbo-spin echo sequence. Acquisition parameters for FLAIR images were set as follows: repetition time, 9,000 ms; echo time, 125 ms; slice thickness, 4 mm; intersection gap, 4 mm; matrix, 256×256; flip angle, 90 degrees. Susceptibility-weighted imaging acquisition was conducted using a turbo 3D gradient echo sequence with a TR=31 ms, TE=7.2, 13.4, 19.6, 25.8 ms, flip angle=17°, field of view=100×100 mm^2, voxel size=0.39×0.39×2 mm^3, and matrix size=512×512×65.

Measurement of WMH of cholinergic pathways

Immunohistochemistry research reveals that the cholinergic pathways in the human brain have origins in the BF and extend to various cortical locations through the medial and lateral cholinergic pathways [20]. The lateral cholinergic pathways traverse the external capsules and claustrum, transmitting signals to the centrum semiovale, ultimately providing supplies to the neocortical regions. Medial cholinergic pathways traverse the cingulum and supply the cingulate and retrosplenial cortices with cholinergic neurotransmitters. Based on these findings, a visual rating scale named the Cholinergic Pathways Hyperintensities Scale (CHIPS) score was proposed to quantify the WMH burden of the cholinergic pathways using conventional MRI [21]. This scale has been recognized as a reliable indicator that better reflects the pathogenesis of cognitive decline by more selectively quantifying WMH in strategic locations rather than only reflecting the volume of WMH [21, 22]. We used an axial T2 FLAIR image to measure the CHIPS score.

The CHIPS were evaluated in four index axial MRI images: the low external capsule, high external capsule, corona radiata, and centrum semiovale (from left to right in Fig. 2, see Additional file 1). The cholinergic pathways were visualized on those reference images with reference to surrounding anatomic landmarks. External capsule, corona radiata, and centrum semiovale were further divided into anterior and posterior portions based on the central point of the corresponding region of interest (red-colored lines in Fig. 2). The severity of WMH was assessed using a visual rating scale with three levels for each region: 0 for normal, 1 for mild (involving less than 50% of the region of interest), and 3 for moderate to severe (involving 50% or more of the region of interest). A weighted number of 4 was assigned to the most densely packed fibers in the low external capsule, while a weighted number of 1 was assigned to the more dispersed fibers in the centrum semiovale (see Additional file 1). Consequently, the maximum CHIPS total score for one cerebral hemisphere is 50 points, and the maximum for both cerebral hemispheres is 100. All scans were assessed with group assignment and clinical information concealed. Two investigators, both board-certified neurologists with four years (YE Kim) and 17 years (J-S Lim) of experience in neuroimaging research, respectively, independently assessed the data, and disagreements between raters were resolved by consensus. The intraclass correlation coefficient (ICC) between the two investigators was 0.942.

Measurement of small vessel disease markers

We evaluated additional small vessel disease (SVD) markers alongside WMH, including lacunes, cerebral microbleeds (CMB), and enlarged perivascular spaces (EPVS). CMBs were assessed on the Microbleed Anatomical Rating Scale for each of the deep, lobar, and infratentorial locations using susceptibility-weighted imaging [23]. EPVS were evaluated in the basal ganglia (BG) and centrum semiovale (CS) regions. Following criteria from previous studies, EPVS were scored as follows: 1 point for 1–10 spaces, 2 points for 11–20 spaces, 3 points for 21–40 spaces, and 4 points for more than 40 spaces [24]. The total SVD score was calculated by assigning 1 point for each of the following: the presence of lacunes, the presence of CMB, deep WMH graded as Fazekas grades 2 or 3 and/or periventricular WMH graded as Fazekas grade 3, and BG PVS with a score of 2 or higher. The points were then summed to derive the total SVD score [25].

Measurement of BF volume

We used the degree of BF atrophy as an indicator for the progression of neurodegeneration caused by cholinergic neuronal loss in patients with cognitive impairment. We performed segmentation of the limbic structure, including BF on 3D T1-weighted MRI, using FreeSurfer toolbox, ScLimbic (v.7.2.0, FMRIB, Oxford, UK) (https://surfer.nmr.mgh.harvard.edu/fswiki/ScLimbic) and obtained the total BF volume as the sum of left and right BF volumes (Fig. 3). After running the scLimbic pipeline, we visually inspected the segmented images, as shown in Fig. 3, to check for any significant errors in structure labelling. We also used the -write_qa_stats function in Freesurfer's scLimbic pipeline to check detailed quality assurance statistics. We then normalized the BF volume by dividing it by the total intracranial volume for subsequent analysis. The MRI sequence used to measure BF volume was acquired simultaneously with the MRI protocol used to measure the CHIPS scores.

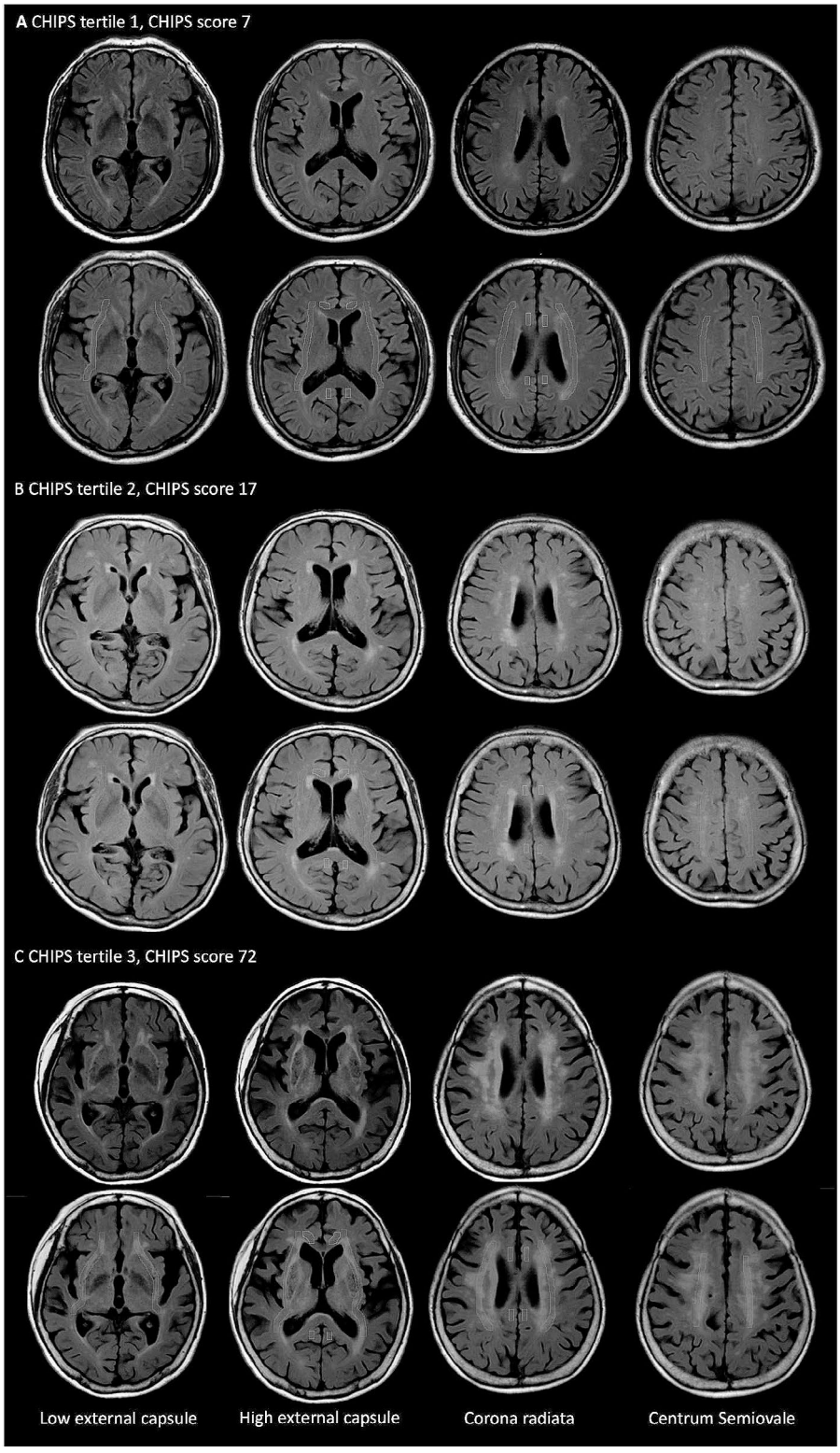

Fig. 2 Representative fluid-attenuated inversion recovery (FLAIR) images of patients in each CHIPS tertile group. In Panels **A** through C, the top row of each panel is the original MRI image, and the bottom row is the image with the region of interest added. Colored lines represent the medial (blue) and lateral (red) cholinergic pathways. The Montreal Neurological Institute (MNI) z-coordinates of the associated index images are about − 1, 10, 25, and 37. Panels **A** through C shows representative FLAIR images of each CHIPS tertile group at the low external capsule, high external capsule, corona radiata, and centrum semiovale levels, from left to right. A represents CHIPSt1 with a CHIPS score of 7, C represents CHIPSt2 with a CHIPS score of 17, and D represents CHIPSt3 with a CHIPS score 72

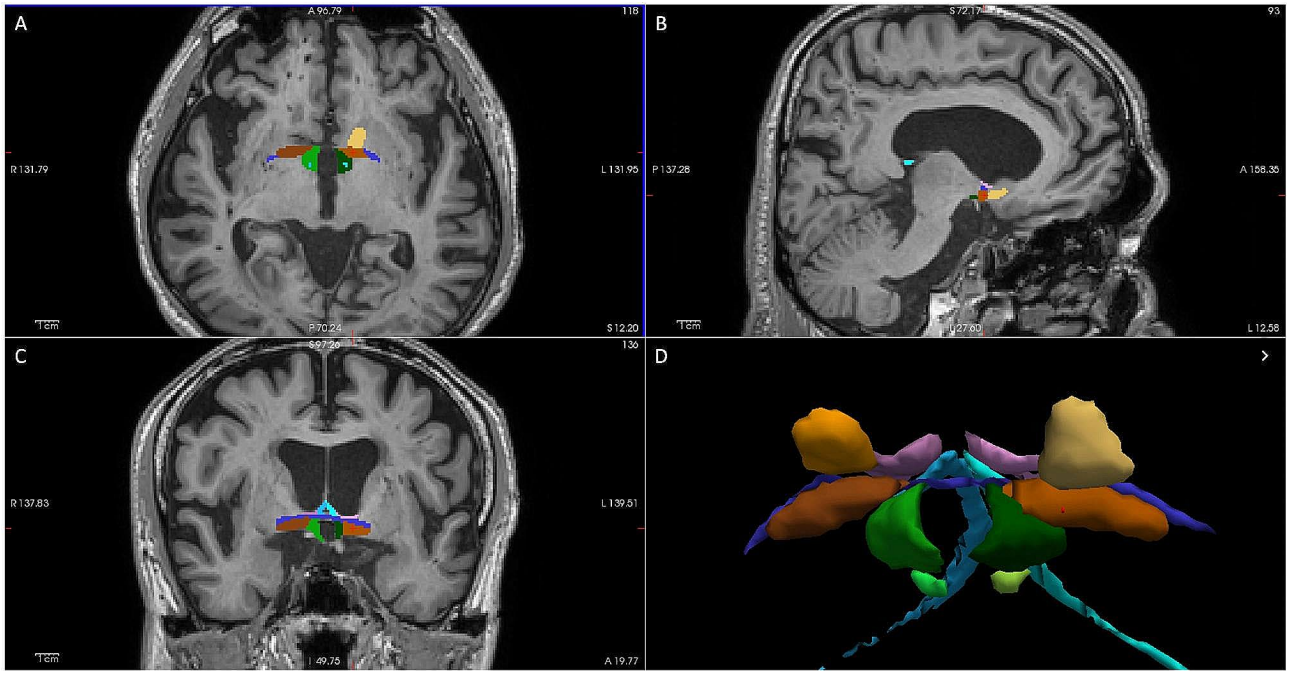

Fig. 3 Segmentation of the basal forebrain using FreeSurfer ScLimbic toolbox. Segmentation of limbic structures including BF was performed using the ScLimbic toolbox from the FreeSurfer toolbox (v.7.2.0, FMRIB, Oxford, UK) (https://surfer.nmr.mgh.harvard.edu/fswiki/ScLimbic). The basal forebrain is marked in brown color in the axial, sagittal, and coronal images of the 3D T1-weighted MRI **(A-C)** and the 3-dimensional reconstruction image **(D)**. Total basal forebrain volume was calculated by adding the volumes of left and right basal forebrains. For subsequent analyses, basal forebrain volume was normalized to head size by dividing it by total intracranial volume

Statistical analyses

We conducted the univariable and multivariable regression to investigate the association between normalized BF volumes and CHIPS scores. All variables were tested for normality (Shapiro-Wilk normality test) and homoscedasticity of variance (Bartlett test), and the CHIPS tertile (CHIPSt) group was included as a categorial variable because CHIPS scores did not satisfy the normal distribution (i.e. CHIPSt1, CHIPSt2, and CHIPSt3 group; with CHIPSt3 had the highest CHIPS score). Pearson's correlation test was conducted between normalized BF volumes and CHIPS scores. In univariable analysis, age at MRI scan, vascular risk factors (e.g., hypertension, diabetes mellitus, hyperlipidemia, coronary artery disease, smoking history), history of stroke, apolipoprotein E (APOE) ε4 status, baseline MMSE, deep and periventricular WMH, lacunes, CMB, EPVS, and total SVD scores were explored [26]. The multivariable regression analysis included all covariates that were significant in the univariable analyses. We assessed multicollinearity using the variance inflation factor (VIF) function from the R (version 4.3.0) car library. A VIF value exceeding 2.5 was considered indicative of potential multicollinearity issues, while a value over 10 was regarded as severe. We also conducted sensitivity analyses to confirm the independent association between normalized BF volume and CHIPS score in the subgroups according to WMH severity (deep WMH graded as Fazekas grades 2 or 3 and/or periventricular WMH graded as Fazekas grade 3). All data analyses were performed using R (version 4.3.0), and a P value <0.05 was considered significant.

Results

From 465 patients with objective cognitive decline who underwent structural brain MRI, ^{18}F-Florbetaben PET, we excluded 261 patients who were confirmed as amyloid positive on ^{18}F-florbetaben PET, 7 patients who had Parkinson's disease dementia, Dementia with Lewy bodies, Progressive Supranuclear Palsy, 7 patients who had brain lesions other than neurodegenerative diseases such as traumatic brain injury or encephalitis, and 3 patients who underwent T1-weighted MRI with a 3 mm slice thickness. Finally, a total of 187 patients were enrolled. The mean age (±standard deviations) was 75.2±5.4 years, and 105 (56.2%) were women. Hypertension was present in 102 (54.5%), a history of stroke in 19 (10.2%), and APOE ε4 carriers in 29 (17.7%). The median scores of the MMSE and education levels were 25 points [IQR 22.0; 27.5] and 12 years [IQR 6.0; 14.0], respectively, and 154 (82.4%), had mild cognitive impairment with a CDR of 0.5. Among the patients with MCI, 80 (42.8% of the total 187 patients) had moderate-to-severe WMH, considered subcortical vascular MCI (Supplemental Table 2). The remaining 74 non-vascular MCI patients included 27

with amnestic MCI (14.4% of the total) and 47 with non-amnestic MCI (25.1% of the total). Among the dementia patients, 21 (11.2% of the total) had moderate-to-severe WMH, deemed as having subcortical vascular dementia. For the remaining 12 dementia patients (6.4% of the total) without or with only mild WMH, diagnoses were as follows: 3 had frontotemporal dementia, 2 had normal pressure hydrocephalus, 1 had posterior cortical atrophy, and 6 were considered other neurodegenerative diseases including limbic-predominant age-related TDP-43 encephalopathy, and argyrophilic grain disease. Using cerebellar gray matter as a reference region, we calculated total cerebral cortical SUVR values, resulting in a median value of 1.17 with an IQR of 1.13 to 1.22. No patients exceeded the cutoff of 1.43.

The median CHIPS score was 12.0 [IQR 5.0; 24.5], with scores in each CHIPS tertile group of 4.0 [2.0; 5.0], 12.0 [9.0; 14.0], and 34.5 [25.0; 42.0] (Table 1). The CHIPSt3 group, which consisted of patients with the highest CHIPS tertile scores, was significantly older ($P=0.02$) and more likely to have hypertension ($P<0.01$) and a history of stroke ($P<0.01$) than the other groups with lower CHIPS scores. Lacune, CMB, and EPVS were all significantly more prevalent in the highest CHIPS tertile group, with 53 (85.5%) having a total SVD score of 2 or more. Figure 2 displays representative FLAIR images of patients in each CHIPS tertile group. Comparing cognitive domain scores across CHIPS tertile groups revealed significant differences in attention, memory, and frontal domain z-scores, with the highest CHIPS tertile group exhibiting decreased cognitive functions in these domains (Table 1, Supplemental Fig. 1). Regarding normalized BF volume, correlations with age- and education-adjusted cognitive domain z-scores indicated significant relationships in all cognitive domains except for attention (Supplemental Fig. 2).

The normalized BF volume of the CHIPSt3 group (% of brain parenchymal volume, mean±SD, 3.52±0.50) was significantly decreased than those of the lower CHIPSt groups (3.71±0.54, CHIPSt2; 3.81±0.55, CHIPSt1; $P<0.01$). In post hoc analysis, the difference in normalized BF volume was significant between the CHIPSt1-CHIPSt3 groups ($P<0.01$) and the CHIPSt2-CHIPSt3 groups ($P<0.01$), but not between the CHIPSt1-CHIPSt2 groups ($P=0.99$) by Tukey honest significant difference test (Fig. 4).

In the univariable regression analysis, factors showing significant associations with the normalized BF volume were the CHIPSt3 group, age, female, education, diabetes mellitus, smoking, previous stroke history, periventricular WMH, and CMB (Table 2). In multivariable regression analysis, the CHIPSt3 group (standardized beta [β_{std}] = -0.25, $P<0.01$), female (β_{std} = 0.20, $P=0.04$), and diabetes mellitus (β_{std} = -0.22, $P<0.01$) showed a significant association with the normalized BF volume (Table 2). Regarding multicollinearity, no variables exceeded a VIF of 2.5.

In sensitivity analyses with subgroups according to WMH severity, a significant negative correlation between CHIPS scores and normalized BF volume in both subgroups with none to mild WMH, (r = -0.28, $p<0.01$) and with moderate to severe WMH (r = -0.42, $p<0.01$) (Fig. 5).

Discussion

We examined the relationship between cholinergic pathway disruption due to strategic WMH and BF volume in a cohort of 187 amyloid-negative neurocognitive disorders. We found a significant decrease in BF volume as a function of higher CHIPS scores after adjusting for potential confounders, including age, hypertension, stroke history, and other SVD markers. These findings imply that WMH in the cholinergic pathway independently contributes to BF atrophy without amyloid pathology.

We hypothesized that the observed results could be attributed to a 'dying-back' phenomenon, in which cortical atrophy is induced by the connecting white matter tract lesion. This mechanism has been suggested in previous studies on multiple sclerosis, having both inflammatory and neurodegenerative aspects [27, 28]. In this cohort of patients, it has been suggested that retrograde neuronal degeneration due to axonal damage within white matter lesions causes cortical atrophy [28]. Studies on stroke patients also indicated a connection between subcortical infarcts and cortical thinning in associated regions, implying secondary neurodegeneration precipitated by axonal disruption [29]. Furthermore, in cerebral small vessel diseases, the progression rate of WMH has been linked to regional cortical atrophy, likely due to secondary downstream denervation [30]. Given the anatomical connectivity between cholinergic neurons in the BF and their projection fibers in the subcortical white matter, white matter lesions, as quantified by CHIPS scoring, would likely contribute to BF volume loss via the 'dying-back' phenomenon.

WMH burden may contribute to cognitive decline and brain atrophy regardless of AD pathology [31, 32]. Studies show that cholinergic deficiency is implicated in VCI [33], but the degree of involvement and underlying mechanisms are still unclear. There are reports that BF atrophy was not observed in VCI; however, these studies did not differentiate between the groups with biomarkers to support the clinical diagnosis [10, 11]. In our study, we limited the study population to patients with negative amyloid PET to eliminate the influence of AD pathology when interpreting the effect

Table 1 Demographic characteristics of study population

Characteristic	Total (*N* = 187)	CHIPSt1 (*N* = 63)	CHIPSt2 (*N* = 62)	CHIPSt3 (*N* = 62)	*P*
CHIPS score, median (IQR)	12 (5.0; 24.5)	4.0 (2.0;5.0)	12.0 (9.0;14.0)	34.5 (25.0;42.0)	< 0.01
Age, years	75.2 ± 5.4	73.8 ± 5.0	75.3 ± 5.6	76.4 ± 5.2	0.02
Female, No. (%)	105 (56.2)	32 (50.8)	38 (61.3)	35 (56.5)	0.50
Education, years	12.0 (6.0; 14.0)	12.0 (6.0;14.0)	10.5 (6.0;16.0)	11.5 (6.0;14.0)	0.89
Medical history, No. (%)					
Hypertension	102 (54.5)	24 (38.1)	35 (56.5)	43 (69.4)	< 0.01
Diabetes mellitus	51 (27.3)	15 (23.8)	17 (27.4)	19 (30.6)	0.69
Hyperlipidemia	73 (39.0)	23 (36.5)	23 (37.1)	27 (43.5)	0.67
Smoking	58 (31.0)	25 (39.7)	18 (29.0)	15 (24.2)	0.16
Previous history of stroke	19 (10.2)	3 (4.8)	4 (6.5)	12 (19.4)	0.01
Previous history of CAD	42 (22.5)	15 (23.8)	13 (21.0)	14 (22.6)	0.93
APOE e4 carriers	29 (17.7)	11 (21.6)	11 (19.3)	7 (12.5)	0.44
Baseline MMSE	25.0 (22.0; 27.5)	27.0 (25.0; 28.0)	25.0 (21.0; 27.0)	24.0 (20.0; 27.0)	< 0.01
Cognitive domain functions					
Attention z-score	-0.28 ± 1.19	-0.05 ± 1.14	-0.09 ± 1.29	-0.72 ± 1.00	< 0.01
Language z-score	-1.11 ± 2.05	-0.89 ± 1.80	-1.21 ± 1.89	-1.23 ± 2.41	0.58
Visuospatial z-score	-1.25 ± 2.16	-0.90 ± 2.04	-1.40 ± 2.15	-1.43 ± 2.26	0.30
Memory z-score	-1.52 ± 1.18	-1.78 ± 1.13	-1.63 ± 1.21	-1.76 ± 1.14	0.02
Frontal z-score	-1.48 ± 1.81	-0.98 ± 1.89	-1.60 ± 1.69	-1.99 ± 1.68	< 0.01
Deep WMH, Fazekas grade 2 or more, median (IQR)	44 (23.5)	0 (0)	9 (14.5)	35 (56.5)	< 0.01
Periventricular WMH, Fazekas grade 3, median (IQR)	38 (20.3)	2 (3.2)	4 (6.5)	32 (51.6)	< 0.01
Lacunes	50 (26.7)	8 (12.7)	16 (25.8)	26 (41.9)	< 0.01
Cerebral microbleeds	81 (43.3)	19 (30.2)	25 (40.3)	37 (59.7)	< 0.01
Deep	46 (24.6)	8 (12.7)	12 (19.4)	26 (41.9)	< 0.01
Lobar	47 (25.1)	11 (17.5)	13 (21.0)	23 (37.1)	0.03
Infratentorial	27 (14.4)	5 (7.9)	7 (11.3)	15 (24.2)	0.02
Enlarged perivascular spaces					
Basal Ganglia					< 0.01
0	4 (2.1)	1 (1.6)	3 (4.8)	0 (0)	
1–10	65 (34.8)	30 (47.6)	16 (25.8)	19 (30.7)	
11–20	85 (45.5)	28 (44.4)	33 (53.2)	24 (38.7)	
20–40	23 (12.3)	3 (4.8)	9 (14.5)	11 (17.7)	
41 or more	10 (5.4)	1 (1.6)	1 (1.6)	8 (12.9)	
Centrum Semiovale					0.03
0	6 (3.2)	1 (1.6)	1 (1.6)	4 (6.5)	
1–10	56 (30.0)	23 (36.5)	10 (16.1)	23 (37.1)	
11–20	65 (34.8)	22 (34.9)	22 (35.5)	21 (33.9)	
20–40	45 (24.1)	15 (23.8)	21 (33.9)	9 (14.5)	
41 or more	15 (8.0)	2 (3.2)	8 (12.9)	5 (8.1)	
Total SVD score					0.18
0	2 (1.1)	0 (0)	1 (1.6)	1 (1.6)	
1	30 (16.0)	13 (20.6)	9 (14.5)	8 (12.9)	
2	85 (45.5)	31 (49.2)	28 (45.2)	26 (41.9)	
3	61 (32.6)	18 (28.6)	23 (37.1)	20 (32.3)	
4	9 (4.8)	1 (1.6)	1 (1.6)	7 (11.3)	
BF volume (x 10^2)	3.71 ± 0.54	3.81 ± 0.55	3.78 ± 0.52	3.52 ± 0.50	< 0.01

Numbers denote mean ± standard deviations or median (IQR) for continuous variables or frequencies (proportions) for categorical variables

Abbreviations: CHIPSt, Cholinergic Pathways Hyperintensities Scale tertile; IQR, interquartile range; CAD, Coronary artery disease; BF, basal forebrain; SVD, small vessel disease

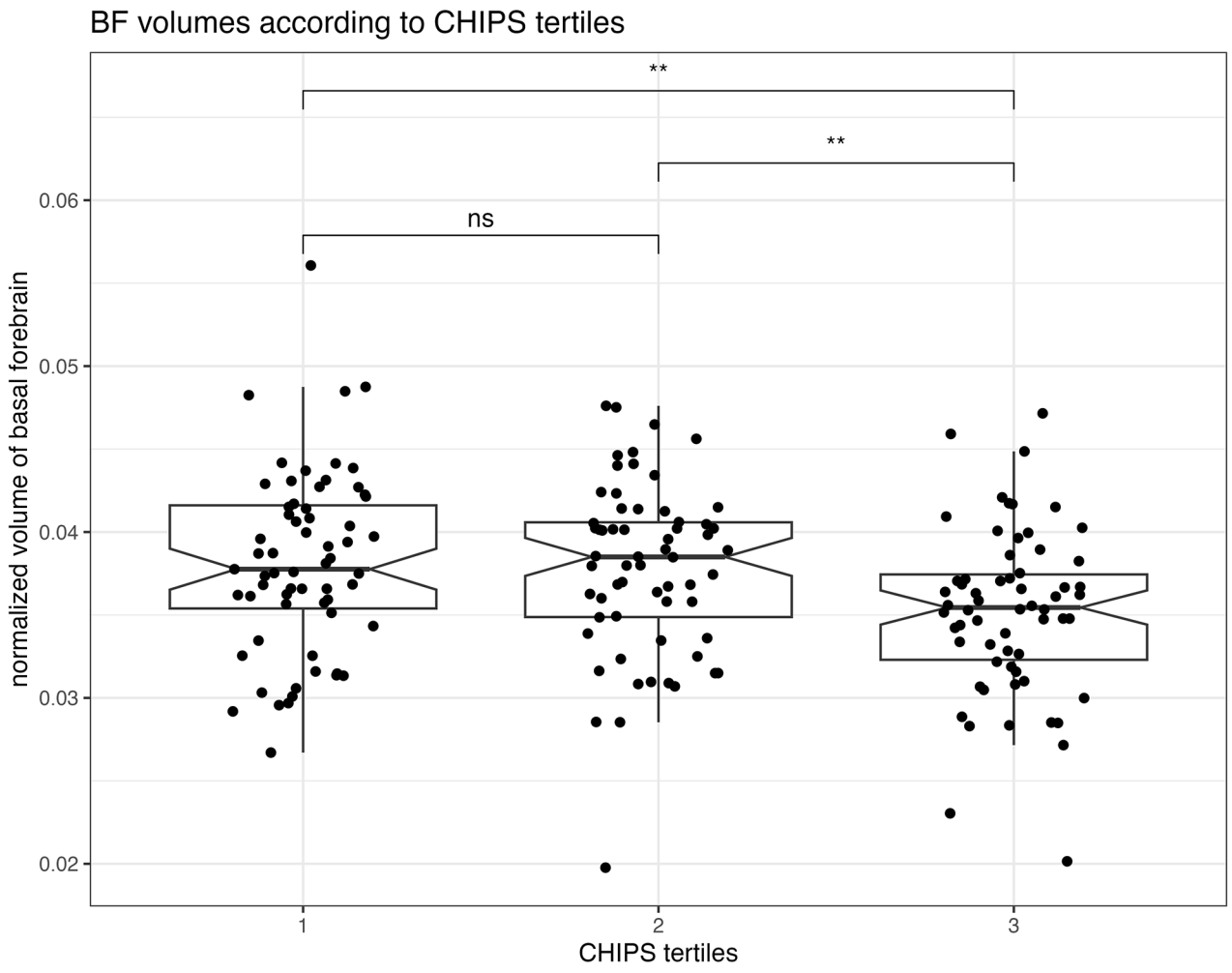

Fig. 4 Differences in BF volume between tertile groups. Box plots show a significant difference in BF volume between tertile groups. The difference in BF volume was significant between the CHIPSt1 and CHIPSt3 groups ($P < 0.01$) and the CHIPSt2 and CHIPSt3 groups ($P < 0.01$), but not between the CHIPSt1 and CHIPSt2 groups ($P = 0.99$). The top and bottom of each box indicate the 75th and 25th percentiles, and the horizontal line inside each box indicates the 50th percentile. P values were obtained using a Tukey test, with an asterisk indicating $P < 0.05$. Abbreviations: BF, basal forebrain; CHIPS, Cholinergic Pathways Hyperintensities Scale; ns, not significant

of cholinergic tract disruption on BF volume. We further excluded patients with Parkinson's disease dementia, Lewy body dementia, and progressive supranuclear palsy, which is known to be accompanied by degeneration of BF neurons and their associated depletion of cortical cholinergic projections as in AD [34, 35]. Thus, our findings suggest that a high WMH burden of cholinergic pathways significantly impacts BF atrophy, even if not caused by amyloid or Lewy body pathologies, which are already known to affect BF volumes.

The pattern of cognitive impairment in our study participants aligns with existing research findings. Previous studies have reported that the cognitive domains most affected in VCI patients are the attention, processing speed, frontal-executive function, and memory domains [36, 37]. Similarly, our analysis found a significant reduction in these domains in the highest tertile CHIPS group (Table 1, Supplemental Fig. 1). The relationship between the BF and cognitive function also showed significant correlations with most cognitive domains, including memory and frontal-executive functions, as reported in the literature (Supplemental Table 2, Supplemental Fig. 2) [2]. These results are expected to broaden our understanding of the interrelationship between WMH in strategic locations, BF volume, and cognitive impairment.

We segmented the BF, but it's crucial to note that this region contains multiple structures. The nbM, which primarily projects to cortical regions, occupies only a small part of the BF. Thus, atrophy measurements of the BF may not accurately reflect cholinergic pathway changes. Research on the nbM is challenging

Table 2 Univariable and multivariable regression analysis for BF volume

	Univariable analysis		Multivariable analysis	
Variable	**Estimate (SE)***	***P*value**	**Estimate (SE)*†**	***P*value**
CHIPSt group				
CHIPSt1	Reference	NA	Reference	NA
CHIPSt2	-0.03 (0.09)	0.72	-2.86 (0.09)	0.71
CHIPSt3	-0.29 (0.09)	< 0.01	-24.51 (0.10)	0.01
Age, years	-0.02 (0.01)	0.03	-10.43 (0.01)	0.13
Female	0.31 (0.08)	< 0.01	20.42 (0.11)	0.04
Education, years	-0.02 (0.01)	< 0.01	-13.59 (0.01)	0.08
Hypertension	-0.05 (0.08)	0.49	NA	NA
Diabetes mellitus	-0.29 (0.09)	< 0.01	-21.74 (0.08)	< 0.01
Hyperlipidemia	0.01 (0.08)	0.92	NA	NA
Smoking	-0.22 (0.08)	0.01	-4.88 (0.10)	0.59
Previous history of stroke	-0.28 (0.13)	0.03	-4.21 (0.12)	0.54
Previous history of CAD	0.04 (0.09)	0.66	NA	NA
APOE ε4 carrier	0.02 (0.11)	0.87	NA	NA
Baseline MMSE	0.01 (0.01)	0.44	NA	NA
Deep WMH, Fazekas grade 2 or more	-0.11 (0.09)	0.23	NA	NA
Periventricular WMH, Fazekas grade 3	-0.20 (0.10)	0.04	8.62 (0.11)	0.29
Lacunes	-0.09 (0.09)	0.33	NA	NA
Cerebral microbleeds	-0.20 (0.08)	0.01	-12.80 (0.08)	0.07
Deep	-0.02 (0.02)	0.25	NA	NA
Lobar	-0.01 (0.02)	0.36	NA	NA
EPVS-BG	-0.04 (0.05)	0.33	NA	NA
EPVS-CS	0.07 (0.04)	0.09	NA	NA
Total SVD scores	0.05 (0.05)	0.27	NA	NA

Estimates and standard error values were expressed by multiplying by 10^2

The multivariable regression analysis included all covariates that were significant in the univariable analyses: CHIPSt, age, female, education, diabetes mellitus, smoking, previous history of stroke, periventricular WMH, cerebral microbleeds

† Standardized beta estimates

Abbreviations: CHIPSt, Cholinergic Pathways Hyperintensities Scale tertile; CAD, Coronary artery disease; MMSE, mini-mental state examination; WMH, white matter hyperintensities; EPVS, enlarged perivascular space; BG, basal ganglia; CS, centrum semiovale; SVD, small vessel disease; SE, Standard error; BF, basal forebrain; NA, not applicable

due to patient-specific variations and the difficulty of accurate segmentation. Manual segmentation, while addressing individual differences, is limited by the nbM's poor visibility on standard 3T T1-weighted MRI. High-resolution 7T MRI offers better accuracy but is not widely available. To mitigate these issues, researchers have developed a probabilistic atlas of the nbM from postmortem histological staining of healthy brains [38]. While this atlas is widely used for its accuracy, it does not capture patient-specific anatomical variability, which is significant given individual differences and disease progression. Recent studies highlight that the probabilistic atlas falls short in accounting for these differences, underscoring the need for better atlas technology. Additionally, deep learning techniques are being investigated to improve segmentation accuracy and address anatomical variability [39]. These methods show promise in improving our understanding of the nbM's role in cognitive impairment, warranting further studies utilizing these advanced techniques.

In our study, diabetes mellitus was the other significant factor affecting BF volume, consistent with previous findings. Diabetes mellitus decreases total and regional brain volume, and longer duration of diabetes mellitus was reported to decrease the volume of the ventral diencephalon, including the BF [40]. A sensitivity analysis of the correlation between CHIPS score and BF volume for diabetes mellitus revealed a significant negative correlation, which can be interpreted as an adverse effect of cholinergic fibers damage on BF volume when there is a disruption of cholinergic pathways due to WMH, independent of the previously known effects of diabetes mellitus. On the other hand, hypertension is also an important determinant in WMH, with high systolic blood pressure contributing to global brain atrophy [41, 42] and low diastolic blood pressure also contributing to brain atrophy [43]. However, it remains to be seen whether hypertension causes BF atrophy, and our results show that the correlation between the two was insignificant.

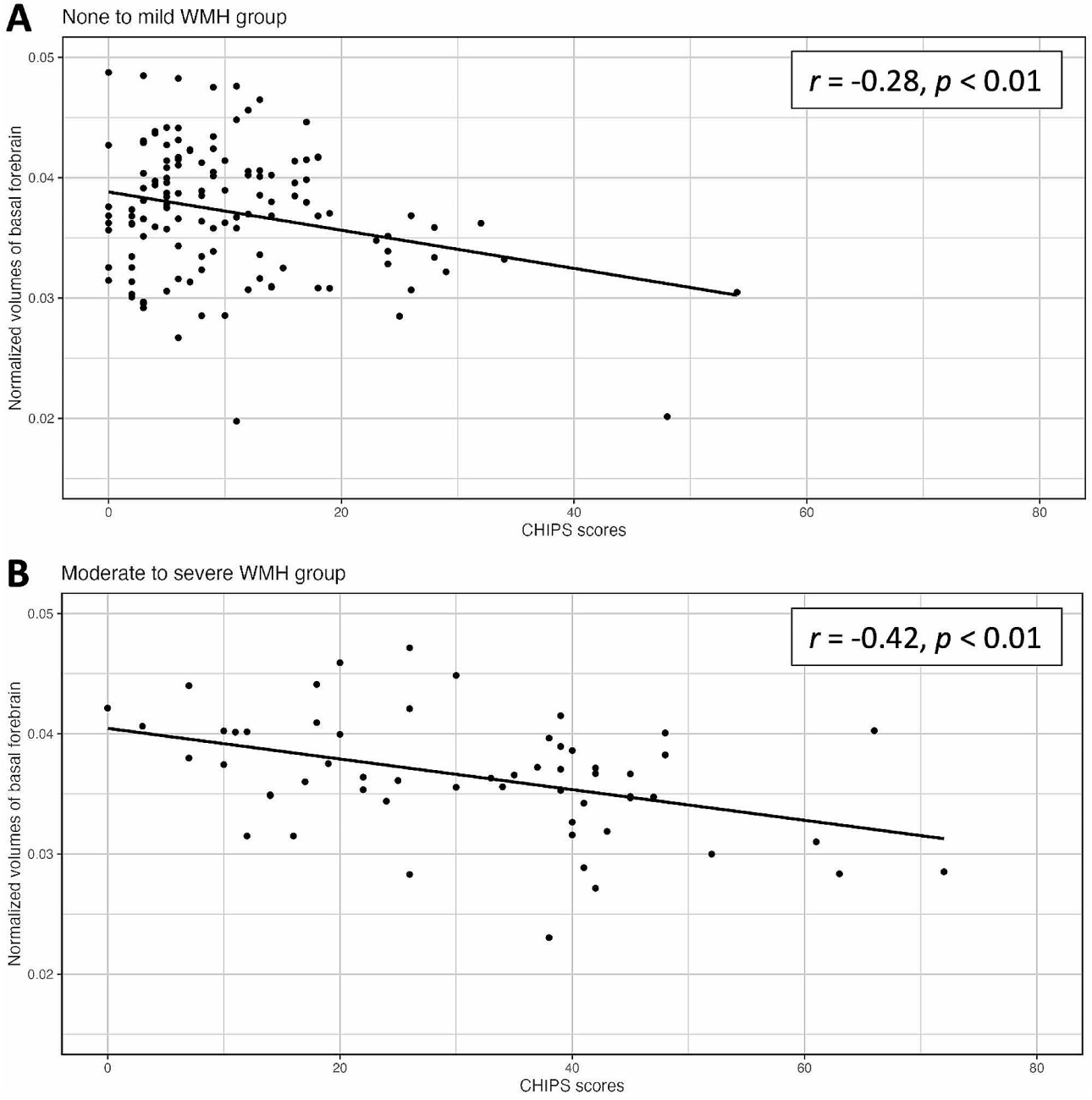

Fig. 5 Sensitivity analysis for the correlations between CHIPS scores and BF volume. The sensitivity analyses examined the relationship between the CHIPS score and the BF volume in subgroups based on WMH severity. The results showed a negative correlation between CHIPS score and normalized BF volume in the subgroup with none to mild WMH **(A)** and with moderate to severe WMH **(B)**

Female sex was the only variable to show a positive correlation with normalized BF volume in the multivariable analysis. There is ongoing debate about the differences in structural brain changes between sexes. Some studies report that female may have structural and functional advantages over male [44], although this is typically confined to periods of healthy aging or MCI. Conversely, when transitioning to dementia, female may experience a faster rate of atrophy [45]. Additionally, during the MCI stage of the AD continuum, previous study suggested that brain atrophy progresses more rapidly in female than in male [46]. Regarding BF volume, it has been observed that female, but not male, show a decrease in BF volume in MCI and AD patients compared to healthy controls [47]. However, these studies did not focus on amyloid-negative patients, making it hard to extrapolate to our study. The sex differences in neurodegenerative

changes remain an actively researched topic, and our findings may serve as valuable reference data for future studies in this area.

In terms of clinical implications, vascular contributions to cognitive impairment and dementia are gaining increasing attention, but no proven treatment exists [48, 49]. In South Korea, the indication for donepezil in vascular dementia was removed in 2019 due to insufficient clinical evidence, leaving patients with very limited pharmacological options. Therefore, elucidating the impact of strategic WMH on BF volume independent of amyloid deposition is essential to guide future therapeutic advancements. Given the findings of cholinergic denervation and reduced choline acetyltransferase activity in patients with VCI, [50, 51] along with clinical observations of treatment responses, it is plausible that a subset of these patients might benefit from acetylcholinesterase inhibitors. Identifying these patients based on the strategic location of WMH could inform target population selection in clinical trials and aid in developing tailored therapeutic strategies.

This study has several limitations and strengths. This is a cross-sectional study, so we cannot assess changes over time, and more research is needed to determine if the observed associations persist prospectively and represent a causal relationship. Longitudinal data may elucidate the additive effects of vascular lesions and neurodegeneration on the progression of cognitive impairment. Additionally, as this study is a single-center, retrospective analysis focusing solely on patients who underwent amyloid PET scans, the study population may be uneven and potentially biased. Consequently, caution is warranted when generalizing these findings to a broader population. Furthermore, the lack of a healthy control group makes it unclear whether the associations reported in this study are specific to cognitive impairment or normal aging. In addition, the potential impact of unmeasured biases not accounted for by the total intracranial volume should also be considered when interpreting our results, even though the BF volume was normalized to total intracranial volume. Finally, this study was not based on accurate quantification of WMH volume within cholinergic pathways using advanced imaging tools, but rather on visual assessment methods, which has inherent limitations on the accuracy of quantification. However, the visual rating method has advantages in terms of applying research findings to actual clinical practice. In hospitals where quantification software is not readily available, the CHIPS visual rating method can be easily utilized, much like the Fazekas scale for WMH or Scheltens' visual grades for medial temporal atrophy [26, 52]. Despite these limitations, the strengths of our study include a well-characterized study population with amyloid PET imaging and a standardized method of measuring BF volume. To our knowledge, this is the first study of the relationship between WMH in cholinergic pathways and BF atrophy in amyloid-negative patients. Our findings may provide a rationale for using acetylcholinesterase inhibitors in amyloid-negative patients with cholinergic pathway involvement and could potentially contribute to developing a tailored therapeutic strategy.

Conclusions

We identified that strategic WMH in the cholinergic pathways, represented by CHIPS scores, was associated with reduced BF volume in cognitively impaired patients with negative amyloid PET scans. Loss of cholinergic neurons in the BF is a cardinal feature of AD, but this study shows that strategic white matter lesions alone contribute to neurodegeneration involving the BF cholinergic neurons.

Abbreviations

AD	Alzheimer's disease
APOE	Apolipoprotein E
BAPL	Brain amyloid plaque load
BF	Basal forebrain
BG	Basal ganglia
CHIPS	Cholinergic pathways hyperintensities scale
CMB	Cerebral microbleeds
CS	Centrum semiovale
EPVS	Enlarged perivascular space
FLAIR	Fluid-attenuated inversion recovery
ICC	Intraclass correlation coefficient
MCI	Mild cognitive impairment
MRI	Magnetic resonance imaging
MMSE	Mini-mental state examination
nbM	nucleus basalis of Meynert
PACS	Picture archiving and communication system
PET	Positron emission tomography
SNSB	Seoul Neuropsychological Screening Battery
SUVR	Standardized value uptake ratio
SVD	Small vessel disease
VCI	Vascular cognitive impairment
VIF	Variance inflation factor
WMH	White matter hyperintensities

Supplementary Information

The online version contains supplementary material available at https://doi.org/10.1186/s13195-024-01536-2.

Supplementary Material 1

Author contributions

J.-S.L. and J.-H.L. conceptualized and designed the study, and also played a key role in the supervision of the project. Y.E.K., J.-S.L., and J.-H.L. were responsible for drafting the manuscript and performing the statistical analysis. All authors contributed to the acquisition, analysis, or interpretation of data. Y.E.K., C.H.S., J.-S.L., and J.-H.L. engaged in critically revising the manuscript for important intellectual content. C.H.S., H.H., J.-S.L., and J.-H.L. provided administrative, technical, or material support. All authors reviewed the manuscript and approved the final version to be published.

Funding
This research was supported by a grant of the Korea Dementia Research Project through the Korea Dementia Research Center (KDRC), funded by the Ministry of Health & Welfare and Ministry of Science & ICT, Republic of Korea. (RS-2024-00344521)

Data availability
The study data are available from the corresponding author upon reasonable request.

Declarations

Ethics approval and consent to participate
Due to the study's retrospective nature and the low risk to participants, the Institutional Review Board of Asan Medical Center approved the protocol and waived patient consent (#2022 – 1010). All methods were performed in accordance with the relevant guidelines and regulations of the Asan Medical Center Ethics Committee and the Declaration of Helsinki.

Consent for publication
Not applicable.

Competing interests
The authors declare no competing interests.

Author details
[1]Department of Neurology, Asan Medical Center, University of Ulsan College of Medicine, Seoul, Korea
[2]Department of Radiology and Research Institute of Radiology, Asan Medical Center, University of Ulsan College of Medicine, Seoul, Korea
[3]Department of Biomedical Sciences, Department of Physiology, Korea University College of Medicine, Seoul, Korea
[4]Department of Neurology, Korea University Anam Hospital, Seoul, Korea
[5]Department of Medical Science and Asan Medical Institute of Convergence Science and Technology, Asan Medical Center, University of Ulsan College of Medicine, Seoul, Korea

Received: 17 March 2024 / Accepted: 16 July 2024
Published online: 15 August 2024

References

1. Chen Z-R, Huang J-B, Yang S-L, Hong F-F. Role of Cholinergic Signaling in Alzheimer's Disease. Molecules. 2022;27:1816.
2. Geula C, Dunlop SR, Ayala I, Kawles AS, Flanagan ME, Gefen T, et al. Basal forebrain cholinergic system in the dementias: vulnerability, resilience, and resistance. J Neurochem. 2021;158:1394–411.
3. Giacobini E, Cuello AC, Fisher A. Reimagining cholinergic therapy for Alzheimer's disease. Brain. 2022;145(7):2250–75.
4. Nemy M, Dyrba M, Brosseron F, Buerger K, Dechent P, Dobisch L, et al. Cholinergic white matter pathways along the Alzheimer's disease continuum. Brain. 2023;146(5):2075–88.
5. Ray NJ, Bradburn S, Murgatroyd C, Toseeb U, Mir P, Kountouriotis GK, et al. In vivo cholinergic basal forebrain atrophy predicts cognitive decline in de novo Parkinson's disease. Brain. 2018;141:165–76.
6. Fernández-Cabello S, Kronbichler M, Dijk KRAV, Goodman JA, Spreng RN, Schmitz TW, et al. Basal forebrain volume reliably predicts the cortical spread of Alzheimer's degeneration. Brain. 2020;143:993–1009.
7. Hall AM, Moore RY, Lopez OL, Kuller L, Becker JT. Basal forebrain atrophy is a presymptomatic marker for Alzheimer's disease. Alzheimers Dement. 2008;4:271–9.
8. Schmitz TW, Spreng RN. Basal forebrain degeneration precedes and predicts the cortical spread of Alzheimer's pathology. Nat Comm. 2016;7:1–13.
9. Teipel SJ, Cavedo E, Hampel H, Grothe MJ, Initiative ADN, (APMI), APMI et al. Basal Forebrain Volume, but Not Hippocampal Volume, Is a Predictor of Global Cognitive Decline in Patients With Alzheimer's Disease Treated With Cholinesterase Inhibitors. Front Neurol. 2018;9:642.
10. Kim H-J, Moon W-J, Han S-H. Differential Cholinergic pathway involvement in Alzheimer's Disease and Subcortical ischemic vascular dementia. J Alzheimer's Dis. 2013;35:129–36.
11. Liu Q, Zhu Z, Teipel SJ, Yang J, Xing Y, Tang Y, et al. White matter damage in the Cholinergic System contributes to cognitive impairment in subcortical vascular cognitive impairment, no dementia. Front Aging Neurosci. 2017;9:47.
12. Auld DS, Kornecook TJ, Bastianetto S, Quirion R. Alzheimer's disease and the basal forebrain cholinergic system: relations to β-amyloid peptides, cognition, and treatment strategies. Prog Neurobiol. 2002;68:209–45.
13. Kar S, Slowikowski SP, Westaway D, Mount HT. Interactions between beta-amyloid and central cholinergic neurons: implications for Alzheimer's disease. J Psychiatry Neurosci. 2004;29:427–41.
14. Kerbler GM, Fripp J, Rowe CC, Villemagne VL, Salvado O, Rose S, et al. Basal forebrain atrophy correlates with amyloid β burden in Alzheimer's disease. Neuroimage Clin. 2015;7:105–13.
15. Ryu HJ, Yang DW. The Seoul Neuropsychological Screening Battery (SNSB) for Comprehensive Neuropsychological Assessment. Dement Neurocognitive Disord. 2023;22:1–15.
16. Johnson KA, Minoshima S, Bohnen NI, Donohoe KJ, Foster NL, Herscovitch P, et al. Appropriate use criteria for amyloid PET: a report of the Amyloid Imaging Task Force, the Society of Nuclear Medicine and Molecular Imaging, and the Alzheimer's Association. Alzheimers Dement. 2013;9:E1–16.
17. Barthel H, Gertz HJ, Dresel S, Peters O, Bartenstein P, Buerger K, et al. Cerebral amyloid-beta PET with florbetaben (18F) in patients with Alzheimer's disease and healthy controls: a multicentre phase 2 diagnostic study. Lancet Neurol. 2011;10(5):424–35.
18. Lee J, Ha S, Kim REY, Lee M, Kim D, Lim HK. Development of amyloid PET analysis Pipeline using deep learning-based brain MRI Segmentation—A comparative validation study. Diagnostics. 2022;12:623.
19. Bullich S, Seibyl J, Catafau AM, Jovalekic A, Koglin N, Barthel H, et al. Optimized classification of 18F-Florbetaben PET scans as positive and negative using an SUVR quantitative approach and comparison to visual assessment. NeuroImage: Clin. 2017;15:325–32.
20. Selden NR, Gitelman DR, Salamon-Murayama N, Parrish TB, Mesulam MM. Trajectories of cholinergic pathways within the cerebral hemispheres of the human brain. Brain. 1998;121:2249–57.
21. Bocti C, Swartz RH, Gao F-Q, Sahlas DJ, Behl P, Black SE. A New Visual Rating Scale to assess Strategic White Matter Hyperintensities within Cholinergic pathways in Dementia. Stroke. 2005;36:2126–31.
22. Behl P, Bocti C, Swartz RH, Gao F, Sahlas DJ, Lanctot KL, et al. Strategic subcortical hyperintensities in cholinergic pathways and executive function decline in treated Alzheimer patients. Arch Neurol. 2007;64:266–72.
23. Gregoire SM, Chaudhary UJ, Brown MM, Yousry TA, Kallis C, Jager HR, et al. The Microbleed Anatomical Rating Scale (MARS): reliability of a tool to map brain microbleeds. Neurology. 2009;73:1759–66.
24. Doubal FN, MacLullich AMJ, Ferguson KJ, Dennis MS, Wardlaw JM. Enlarged Perivascular spaces on MRI are a feature of Cerebral Small Vessel Disease. Stroke. 2010;41:450–4.
25. Staals J, Makin SDJ, Doubal FN, Dennis MS, Wardlaw JM. Stroke subtype, vascular risk factors, and total MRI brain small-vessel disease burden. Neurology. 2014;83:1228–34.
26. Fazekas F, Kleinert R, Offenbacher H, Schmidt R, Kleinert G, Payer F, et al. Pathologic correlates of incidental MRI white matter signal hyperintensities. Neurology. 1993;43:1683–1683.
27. Andravizou A, Dardiotis E, Artemiadis A, Sokratous M, Siokas V, Tsouris Z, et al. Brain atrophy in multiple sclerosis: mechanisms, clinical relevance and treatment options. AutoImmun Highlights. 2019;10:1–25.
28. Siffrin V, Vogt J, Radbruch H, Nitsch R, Zipp F. Multiple sclerosis–candidate mechanisms underlying CNS atrophy. Trends Neurosci. 2010;33:202–10.
29. Duering M, Righart R, Csanadi E, Jouvent E, Hervé D, Chabriat H, et al. Incident subcortical infarcts induce focal thinning in connected cortical regions. Neurology. 2012;79:2025–8.
30. Lambert C, Benjamin P, Zeestraten E, Lawrence AJ, Barrick TR, Markus HS. Longitudinal patterns of leukoaraiosis and brain atrophy in symptomatic small vessel disease. Brain. 2016;139:1136–51.
31. Cao Z, Mai Y, Fang W, Lei M, Luo Y, Zhao L, et al. The correlation between White Matter Hyperintensity Burden and Regional Brain Volumetry in patients with Alzheimer's Disease. Front Hum Neurosci. 2022;16:760360.
32. Berg EVD, Geerlings MI, Biessels GJ, Nederkoorn PJ, Kloppenborg RP. White matter hyperintensities and cognition in mild cognitive impairment and Alzheimer's disease: a domain-specific meta-analysis. J Alzheimers Dis. 2018;63:515–27.
33. Tohgi H, Abe T, Kimura M, Saheki M, Takahashi S. Cerebrospinal fluid acetylcholine and choline in vascular dementia of Binswanger and multiple small

infarct types as compared with Alzheimer-type dementia. J Neural Transm. 1996;103:1211–20.
34. Gan C, Cao X, Wang L, Sun H, Ji M, Zhang H, et al. Cholinergic basal forebrain atrophy in Parkinson's disease with freezing of gait. Ann Clin Transl Neurol. 2023;10(5):814–24.
35. Grothe MJ, Schuster C, Bauer F, Heinsen H, Prudlo J, Teipel SJ. Atrophy of the cholinergic basal forebrain in dementia with Lewy bodies and Alzheimer's disease dementia. J Neurol. 2014;261:1939–48.
36. Lanctôt KL, Lindsay MP, Smith EE, Sahlas DJ, Foley N, Gubitz G et al. Canadian Stroke Best Practice Recommendations: Mood, Cognition and Fatigue following Stroke, 6th edition update 2019. Int J Stroke. 2019;15:668–88.
37. Sachdev P, Kalaria R, O'Brien J, Skoog I, Alladi S, Black SE, et al. Diagnostic Criteria for Vascular Cognitive disorders. Alz Dis Assoc Dis. 2014;28:206–18.
38. Zaborszky L, Hoemke L, Mohlberg H, Schleicher A, Amunts K, Zilles K. Stereotaxic probabilistic maps of the magnocellular cell groups in human basal forebrain. NeuroImage. 2008;42:1127–41.
39. Doss DJ, Johnson GW, Narasimhan S, Shless JS, Jiang JW, González HFJ, et al. Deep learning segmentation of the Nucleus Basalis of meynert on 3T MRI. Am J Neuroradiol. 2023;44:1020–5.
40. Zhang W, Lu J, Qing Z, Zhang X, Zhao H, Bi Y, et al. Effects of Subcortical Atrophy and Alzheimer's Pathology on Cognition in Elderly Type 2 diabetes: the Alzheimer's Disease Neuroimaging Initiative Study. Front Aging Neurosci. 2022;14:781938.
41. Firbank MJ, Wiseman RM, Burton EJ, Saxby BK, O'Brien JT, Ford GA. Brain atrophy and white matter hyperintensity change in older adults and relationship to blood pressure. J Neurol. 2007;254:713.
42. Petrovitch H, White LR, Izmirilian G, Ross GW, Havlik RJ, Markesbery W, et al. Midlife blood pressure and neuritic plaques, neurofibrillary tangles, and brain weight at death: the HAAS. Honolulu-Asia aging study. Neurobiol Aging. 2000;21:57–62.
43. Jochemsen HM, Muller M, Visseren FL, Scheltens P, Vincken KL, Mali WP, et al. Blood pressure and progression of brain atrophy: the SMART-MR Study. JAMA Neurol. 2013;70:1046–53.
44. Baik K, Jeon S, Yang S-J, Na Y, Chung SJ, Yoo HS, et al. Cortical thickness and brain glucose metabolism in healthy aging. J Clin Neurol. 2023;19:138–46.
45. Cieri F, Zhuang X, Cordes D, Kaplan N, Cummings J, Caldwell J, et al. Relationship of sex differences in cortical thickness and memory among cognitively healthy subjects and individuals with mild cognitive impairment and Alzheimer disease. Alzheimer's Res Ther. 2022;14:36.
46. Ferretti MT, Iulita MF, Cavedo E, Chiesa PA, Dimech AS, Chadha AS, et al. Sex differences in Alzheimer disease — the gateway to precision medicine. Nat Rev Neurol. 2018;14:457–69.
47. Shi Y, Cui D, Sun F, OuYang Z, Dou R, Jiao Q, et al. Exploring sexual dimorphism in basal forebrain volume changes during aging and neurodegenerative diseases. iScience. 2024;27:109041.
48. Gladman JT, Corriveau RA, Debette S, Dichgans M, Greenberg SM, Sachdev PS, et al. Vascular contributions to cognitive impairment and dementia: research consortia that focus on etiology and treatable targets to lessen the burden of dementia worldwide. Alzheimer's Dement: Transl Res Clin Interv. 2019;5:789–96.
49. Gorelick PB, Scuteri A, Black SE, Decarli C, Greenberg SM, Iadecola C, et al. Vascular contributions to cognitive impairment and dementia. Stroke. 2011;42:2672–713.
50. Mesulam M, Siddique T, Cohen B. Cholinergic denervation in a pure multiinfarct state. Neurology. 2003;60:1183–5.
51. Keverne JS, Low WCR, Ziabreva I, Court JA, Oakley AE, Kalaria RN. Cholinergic neuronal deficits in CADASIL. Stroke. 2007;38:188–91.
52. Scheltens P, Leys D, Barkhof F, Huglo D, Weinstein HC, Vermersch P, et al. Atrophy of medial temporal lobes on MRI in probable Alzheimer's disease and normal ageing: diagnostic value and neuropsychological correlates. J Neurol Neurosurg Psychiatry. 1992;55:967.

Publisher's Note